Available online at www.sciencedirect.com
ScienceDirect
Applied Catalysis B: Environmental 80 (2008) 42–50
APPLIED CATALYSIS B: ENVIRONMENTAL
www.elsevier.com/locate/apcatb

Solar photo-Fenton degradation of Reactive Blue 4 in a CPC reactor

A. Durán *, J.M. Monteagudo, E. Amores

Department of Chemical Engineering, Escuela Técnica Superior de Ingenieros Industriales, University of Castilla-La Mancha, Avda. Camilo José Cela 3, 13071 Ciudad Real, Spain

Received 10 October 2007; received in revised form 15 November 2007; accepted 20 November 2007
Available online 22 November 2007

Abstract

Solar photo-Fenton and solar photo-Fenton–ferrioxalate processes using a compound parabolic collector (CPC) were applied to the degradation of Reactive Blue 4 (RB4) solutions, proving to be an efficient method. Multivariate experimental design (including the following variables: pH and initial concentrations of Fe(II), oxalic acid, H_2O_2 and RB4) was used. The efficiency of photocatalytic degradation was determined from the analysis of the following parameters: color removal, total organic carbon (TOC) and chemical oxygen demand (COD). The decoloration rate pseudoconstant was calculated as a function of the accumulated solar energy received by the water solution.

Experimental data were fitted using neural networks (NNs) which reproduce experimental data within 86% of confidence and allows the simulation of the process for any value of parameters in the experimental range studied. Analysis of dissolved H_2O_2 during reaction also helps to explain the scavenger effect and the dye mineralization grade.

The solar photo-Fenton–ferrioxalate process increases degradation rate of RB4 since ferrioxalate complexes absorb strongly and a higher portion of the solar spectrum can be used. Although the addition of oxalic acid increases operating costs, it improves the process and it also helps to reduce pH in solution, decreasing charges derived from this operation. Under the optimum conditions, ($[H_2O_2]$ = 120 ppm (in two additions), [Fe(II)] = 7 ppm, $[(COOH)_2]$ = 10 ppm, pH 2.5), color and COD were completely removed whereas TOC was reduced up to 66%.

Keywords: Dye; Ferrioxalate; Neural networks; Mineralization; Textile wastewater

1. Introduction

Textile industry in one of the highest water consuming sectors. After dying, more than 15% of the dyes are lost in wastewater streams [1]. These effluents have recently been proven to be degraded efficiently by a variety of homogeneous and heterogeneous advanced oxidation processes (AOPs) [2].

Among them, aqueous degradation of the commonly used textile dye Reactive Blue 4 (RB4) has already been studied using heterogeneous catalysts such us TiO_2 and ZnO combined with artificial UV or solar light sources [3–5], electrochemical techniques [6,7], or homogeneous UV/Fenton [8].

The main advantage of Fenton's reaction compared to other AOPs is that the process offers a cost effective source of hydroxyl radicals and it is easy to operate and maintain [9]. Photo-Fenton process combines Fenton and UV–vis light. Under these conditions the photolysis of Fe(III) complexes allows Fe(II) regeneration. This process is of special interest because solar light can be used as energy source [10]. Among solar collector systems, compound parabolic collectors (CPCs) are a good option for solar photochemical applications [11], since they can make highly efficient use of both direct and diffuse solar radiation without the need for solar tracking [12]. CPCs have a reflective surface that concentrates the radiation on a tubular receiver located in the focus of the parabola.

On the other hand, the use of ferrioxalates in the degradation of organic pollutants using solar light has been reported to be effective [13–15] since a higher portion of the solar spectrum can be used. The photolysis of ferrioxalate generates Fe(II) in acid solutions through a well known mechanism [16,17], improving degradation rate. Absorption of a photon by an Fe(III)–polycarboxylate species initiates the formation of short-lived intermediates that ultimately yield Fe(II) and a free polycarboxylate radical [18]. At pH 3, the

* Corresponding author. Tel.: +34 926295300x3814; fax: +34 926295361.
E-mail address: Antonio.Duran@uclm.es (A. Durán).

0926-3373/$ – see front matter © 2007 Elsevier B.V. All rights reserved.
doi:10.1016/j.apcatb.2007.11.016

intermediate oxalate radical reacts with molecular oxygen and generates the hydroperoxyl radical ($O_2^{\bullet -}$) which disproportionates to form H_2O_2. Hence, the photolysis of ferrioxalate in the presence of H_2O_2 is a continuous source of Fenton's reagent. Furthermore, the irradiation of ferric ions in the presence of carboxylic acids (including oxalic acid) induces the oxidation of the acid releasing carbon dioxide [19]. Among the low molecular weights polycarboxylates acids, oxalic acid is one of the most active acids in photo-Fenton-like reaction [20].

On the other hand, although the addition of oxalic acid increases overall operating costs, it improves degradation rate and it also helps to reduce pH in solution.

Degradation of Reactive Blue 4 using a photo-Fenton process under solar irradiation has recently been reported [2]. However, the experimental set-up consisted on a discontinue small glass vessel exposed to direct sunlight without stirring. Moreover, experimental variables were not optimized with the consequent Fe precipitation, radiation was only measured at 365 nm and H_2O_2 was not measured during reaction. Even so, the authors have demonstrated that solar light is a feasible technique for the dye degradation. The research presented in this paper using a CPC, multivariate experimental design and neural networks to fit data accounts for a number of important advantages such as:

(a) CPC allows a continuous treatment of wastewater being an industrially feasible technique [11]. It is also more efficient than direct sun exposition since all the radiation that reaches the aperture area of the CPC (not only direct) can be collected and redirected to the reactor.
(b) The central composite design allows to study the effect of all the variables simultaneously (pH and initial concentrations of Fe(II), oxalic acid, H_2O_2 and RB4), and the later fitting with NNs permits to obtain optimum operating conditions based on the kinetic mechanism. Additionally, the saliency analysis of each variable in the NN helps to discern the real relevance of all of them.
(c) The analysis of H_2O_2 remaining in solution during degradation helps to understand the scavenger effect of this compound.
(d) The use of a pseudokinetic rate constant (based on the accumulated solar energy) allows to compare all the experiments, unaware of the time required to receive the radiation, which is different depending on ambient and climatological conditions (sunny or cloudy day).

2. Experimental

2.1. Materials

Analytical grade ferrous sulfate ($FeSO_4 \cdot 7H_2O$), oxalic acid $(COOH)_2 \cdot 2H_2O$ and 30% hydrogen peroxide (H_2O_2) were purchased from Panreac and used as received. RB4 ($C_{23}H_{14}Cl_2N_6O_8S_2$) solutions were prepared from pure compound purchased from Aldrich. pH was previously adjusted (between 2 and 12) by using H_2SO_4 and NaOH solutions.

2.2. Photochemical reactions

The CPC is composed by a solar reactor (50 L) that consists of a continuously stirred tank, a centrifugal recirculation pump, a solar collector unit with an area of 2 m^2 (concentration factor = 1) in an aluminium frame mounted on a fixed south-facing platform tilted 45° in Ciudad Real (Spain) and connecting tubing and valves (Fig. 1). This solar unit has 16 borosilicate-glass tubes (OD 32 mm, transmissivity > 50% at $\lambda > 300$ nm; >75% at $\lambda > 320$ nm; >90% at (> 350 nm) connected by plastic joints, and the total illuminated volume inside the absorber tubes is 16 L. Solar ultraviolet radiation

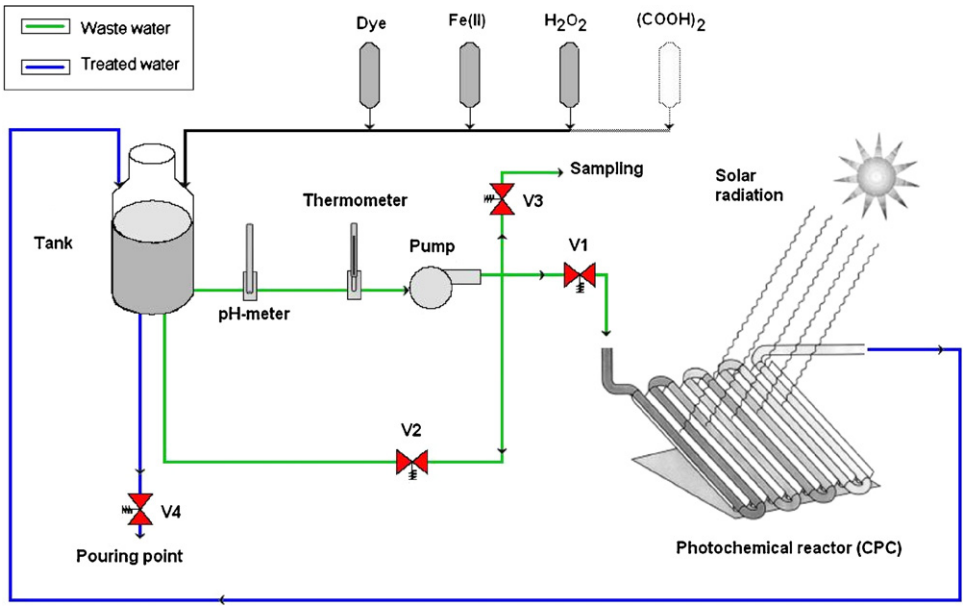

Fig. 1. Experimental set-up based on a CPC.

(400–600 nm) and UV radiation (200–400 nm) were measured by two radiometers Ecosystem model ACADUS which provide data in terms of incident solar power, Wm^{-2}, and accumulated solar power, W h.

2.3. Analysis

Color removal was determined by UV absorption at 594 nm using a UV–vis spectrophotometer (Zuzi 4418PC). The mineralization grade of RB4 was evaluated by determination of total organic carbon concentration using a TOC analyzer (TOC-5000A Shimadzu).

Evolution of the concentration of H_2O_2 in solution was obtained by titration through an aqueous solution of potassium permanganate (0.02 mol L^{-1}) using an automatic Titrino SET/MET 702 (Metrohm).

Chemical oxygen demand (COD, ppm O_2/L) analyses were performed by using the ''Closed Reflux Colorimetric Method''. Samples were refluxed in strongly acidic solution with a known excess of potassium dichromate (VI). The oxygen consumed was measured using a calibration curve with a spectrophotometer (HACH, DR-2000).

2.4. Experimental design

The central composite experimental design was applied to investigate the effect of different variables for each process:

(a) Solar photo-Fenton: pH and initial concentrations of Fe(II), H_2O_2 and RB4.
(b) Solar photo-Fenton–ferrioxalate: pH and initial concentrations of Fe(II), oxalic acid and H_2O_2.

Each design consists of three series of experiments [21]:

(i) a factorial design 2^k (all possible combinations of codified values +1 and −1) which in the case of $k = 4$ variables consists of 16 experiments,
(ii) axial of star points (codified values $\alpha = 2^{k/4} = \pm 2.378$) consisting of $2k = 8$ experiments, and
(iii) central, replicates of the central point (4 experiments)

Table 1
Mulivariate experimental design matrix for the study of RB4 degradation under the processes: solar photo-Fenton and solar photo-Fenton–ferrioxalate

Experiment	Solar photo-Fenton				Solar photo-Fenton–ferrioxalate			
	$[H_2O_2]$ (ppm)	[Fe] (ppm)	pH	[RB4] (ppm)	$[H_2O_2]$ (ppm)	[Fe] (ppm)	pH	$[(COOH_2)]$ (ppm)
1	450	11.25	9.5	25	240	5.75	4.25	45
2	150	11.25	9.5	25	120	5.75	4.25	45
3	450	3.75	9.5	25	240	3.25	4.25	45
4	150	3.75	9.5	25	120	3.25	4.25	45
5	450	11.25	4.5	25	240	5.75	2.75	45
6	150	11.25	4.5	25	120	5.75	2.75	45
7	450	3.75	4.5	25	240	3.25	2.75	45
8	150	3.75	4.5	25	120	3.25	2.75	45
9	450	11.25	9.5	15	240	5.75	4.25	15
10	150	11.25	9.5	15	120	5.75	4.25	15
11	450	3.75	9.5	15	240	3.25	4.25	15
12	150	3.75	9.5	15	120	3.25	4.25	15
13	450	11.25	4.5	15	240	5.75	2.75	15
14	150	11.25	4.5	15	120	5.75	2.75	15
15	450	3.75	4.5	15	240	3.25	2.75	15
16	150	3.75	4.5	15	120	3.25	2.75	15
17	600	7.5	7	20	300	4.5	3.5	30
18	0	7.5	7	20	60	4.5	3.5	30
19	300	15	7	20	180	7	3.5	30
20	300	0	7	20	180	2	3.5	30
21	300	7.5	12	20	180	4.5	5	30
22	300	7.5	2	20	180	4.5	2	30
23	300	7.5	7	30	180	4.5	3.5	60
24	300	7.5	7	10	180	4.5	3.5	0
25	300	7.5	7	20	180	4.5	3.5	30
26	300	7.5	7	20	180	4.5	3.5	30
27	300	7.5	7	20	180	4.5	3.5	30
28	300	7.5	7	20	180	4.5	3.5	30
	Levels				Levels			
(+α)	600	15	12	30	300	7	5	60
(−α)	0	0	2	10	60	2	2	0
(+1)	450	11.25	9.5	25	240	5.75	4.25	45
(−1)	150	3.75	4.5	15	120	3.25	2.75	15
(0)	300	7.5	7	20	180	4.5	3.5	30

The temperature was not controlled during the experiment, but it was measured during reaction, so that the average temperature was included in the fitting. It was found that the initial rate of decoloration of RB4 obeys pseudo-first order kinetics. The values of k_d (decoloration rate pseudoconstant, $W^{-1}\,h^{-1}$) were related to the accumulated energy received by the solution.

2.5. Neural network strategy

In this work, a linear basis function (linear combination between inputs, X_j, and weight factors, W_{ij}) was used:

$$U_i = \sum_{j=1}^{n} W_{ij} X_j \quad (1)$$

Each neural network is solved with two neurones and uses a simple exponential activation function [22]:

$$f(U_i) = \frac{1}{1 + e^{-U_i}} \quad (2)$$

The strategy is based on a back propagation calculation. Parameters are found using the solver tool in an in-house Excel spreadsheet and using the Marquardt non-linear fitting algorithm [23]. Further details can be found in literature [8]. Finally, a measure of the saliency of the input variables was made based upon the connection weights of the NNs [24]. This study allows analysis of the relevance of each variable with respect to the others (expressed as a percentage).

3. Results and discussion

3.1. Solar photo-Fenton process

The complete experimental design matrix and variables range for this process are shown in Table 1.

Experimental results and NNs predictions are shown in Fig. 2 and are in good agreement, with an average error lower than 12% for the decoloration rate pseudoconstant (k_d). The equation and parameters of the fitting are shown in Table 2. N_1 and N_2 are general factors related to the first and the second neuron, respectively. W_{11} to W_{15} are the contribution parameters to the first neuron and represent the influence of each of the five variables in the process ([H_2O_2], [Fe(II)], [RB4], pH and temperature); W_{21} to W_{25} are the contributions to the second neuron and are related to the same variables.

The results of a saliency analysis on the input variables for each neural network (%) are shown in Table 3. From these results it is possible to deduce the effect of each parameter on the variable studied. It is confirmed that pH, [Fe(II)] and [H_2O_2] are the most significant factors affecting the decoloration kinetics of the process, as will be explained below.

3.1.1. Effect of H_2O_2 and Fe(II) initial concentrations

The equation shown in Table 2 allows a simulation analysis of the effect of any of the studied variables on the value of k_d. For example, the influence of the initial concentration of H_2O_2 and Fe(II) is represented in three dimensions in Fig. 3 (simulation conditions: $T = 20\ ^\circ C$, [RB4] = 20 ppm, pH 3).

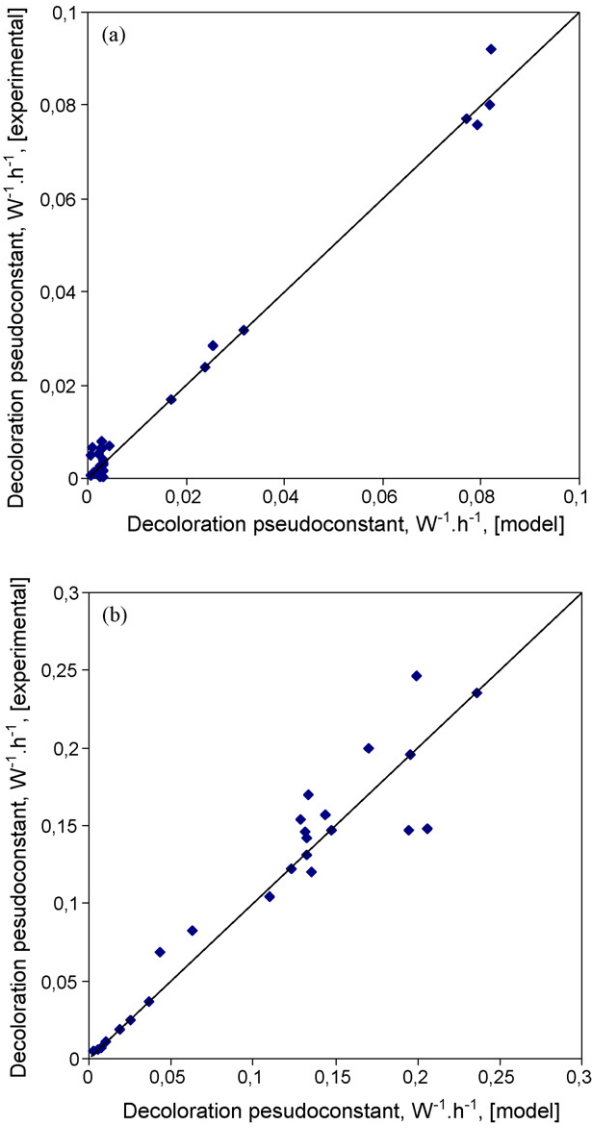

Fig. 2. Neural network fittings of the decoloration rate pseudoconstant. (a) solar photo-Fenton process; (b) solar photo-Fenton–ferrioxalate process.

Results show that k_d increases with initial Fe(II) concentration until reaching a maximum value when a low concentration of H_2O_2 is used (<300 ppm). This can be explained with the kinetic photo-Fenton mechanism shown in Table 4 (from ref. [8]).

It is well known that an increase in H_2O_2 concentration produces a higher amount of $^\bullet$OH radicals (reactions 1 and 18 in Table 4) responsible for RB4 destruction. However, an excess of hydrogen peroxide reduces catalytic activity since it favors reaction 3 (where $^\bullet$OH reacts with peroxide), reducing the amount of radicals available to destroy RB4 and producing the *scavenger effect*. Additionally, decomposition of hydrogen peroxide to form water and oxygen (reactions 3 + 13 + 17) is also favored.

Fig. 4 shows an example of the effect of initial Fe(II) concentration on hydrogen peroxide remaining in solution for

Table 2
Equation and parameters of neural network fittings for RB4 degradation under the processes: solar photo-Fenton and solar photo-Fenton–ferrioxalate

Neural network fitting			
Equation	$k_d\ [W^{-1}\ h^{-1}] = N_1(1/(1 + 1/\mathrm{Exp}(PW_{11} + FW_{12} + RW_{13} + HW_{14} + TW_{15}))) + N_2(1/(1 + 1/\mathrm{Exp}(PW_{21} + FW_{22} + RW_{23} + HW_{24} + TW_{25})))$		
Weight factors	Parameter	Solar photo-Fenton	Solar photo-Fenton–ferrioxalate
N_1	Neurone	0.0030	0.2203
W_{11}	$[H_2O_2]$	4.6144	−1.1565
W_{12}	[Fe (II)]	−8.4103	7.6317
W_{13}	[RB4]	4.4969	–
W_{13}	$[(COOH)_2]$	–	1.2449
W_{14}	pH	−1.7417	−3.5383
W_{15}	Temperature	8.8915	−5.9403
N_2	Neurone	0.0819	0.1301
W_{21}	$[H_2O_2]$	−13.0554	2.3166
W_{22}	[Fe (II)]	15.0133	−9.3156
W_{23}	[RB4]	−32.9172	–
W_{23}	$[(COOH)_2]$	–	−64.6704
W_{24}	pH	−4.1370	40.9054
W_{25}	Temperature	13.6780	20.0649

Parameters values (P, F, R, H and T) in equations must be previously normalized to the (0.1) interval. P = initial concentration of hydrogen peroxide, ppm; F = initial concentration of Fe(II), ppm; R = initial concentration of Reactive Blue 4 for the solar photo-Fenton process or $[(COOH)_2]$ for the solar photo-Fenton–ferrioxalate process, ppm; H = pH, T = Temperature, (°C).

this process (initial conditions: $[H_2O_2]$ = 150ppm, [RB4] = 15 ppm, pH 4.5, T = 20 °C). When initial concentration of Fe(II) is low (3.75 ppm), the amount of H_2O_2 remaining in solution is always very high showing that this reactive is in excess causing the above mentioned scavenger effect. That is the reason why an increase in the initial H_2O_2 concentration always leads to a decrease in k_d (Fig. 3). However, when the concentration of Fe(II) is high (11.25 ppm), the amount of H_2O_2 in solution is very low after 20 W h of accumulated solar energy, so that the initial concentration of hydrogen peroxide can be increased up to 300 ppm without suffering the scavenger effect.

3.1.2. Effect of pH

As literature reports, wastewater treatment with Fenton or photo-Fenton processes is highly pH dependent [25–30]. In previous studies, Durán et al. [8] found a high RB4 decoloration rate at basic pH when the initial $[H_2O_2]$ was high under artificial UV photo-Fenton treatment.

Epolito et al. [31] predicted three predominant deprotonated unhydrolyzed RB4 species between the pH values found

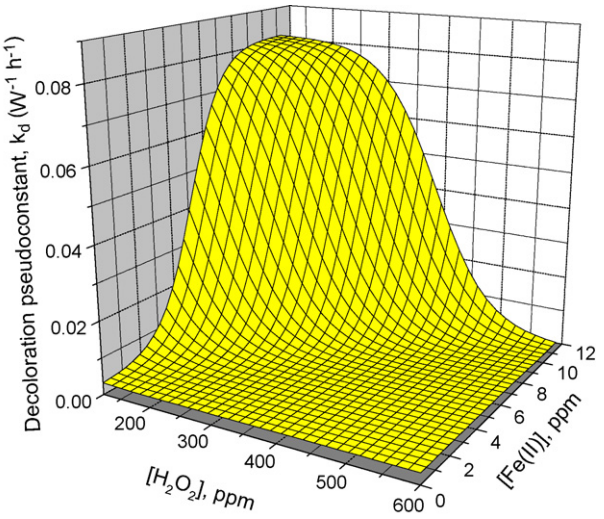

Fig. 3. NNs simulation of the effect of influence of the initial concentration of H_2O_2 and Fe(II) on k_d for the photo-Fenton process (conditions: pH 3, T = 20 °C, [RB4] = 20 ppm).

in the environment, which can have different reactivity. Consequently, different decoloration processes may have different optimal pH values. In this case, solar radiation (with a different emission spectra than artificial UV lamps) produces photolysis of peroxide at a slower rate than UV radiation, so that this compound is nearly always in excess in solution (as previously explained) and low concentrations must be used to avoid the scavenger effect. Under these conditions, it was found that acidic pHs (2–3) produced a faster decoloration during the solar photo-Fenton process. This can be seen in Fig. 5 (simulation obtained from NNs fitting equation) where the effect of pH on the value of decoloration pseudoconstant, k_d is shown (initial conditions: [Fe(II)] = 11.25 ppm, [RB4] = 20 ppm, T = 20 °C).

3.1.3. Mineralization under the optimum conditions (solar photo-Fenton)

A long experiment monitoring TOC, COD, color and H_2O_2 in solution was made under optimun conditions selected from NNs ($[H_2O_2]$ = 100 ppm, [Fe(II)] = 9.4 ppm, [RB4] = 25 ppm, pH 2). Results are shown in Fig. 6. 100% of decoloration was obtained whereas 82% and 23% of COD and TOC removal respectively were reached. TOC reduction is due to the decarboxylation of organic-acid intermediates [32]:

$$[Fe^{(III)}(RCO_2)^-]^{+2} \rightarrow Fe^{(II)} + CO_2 + R^\bullet \quad (3)$$

However it is remarkable to mention that when the accumulated solar energy is 150 W h, hydrogen peroxide in solution has

Table 3
Saliency analysis of the input variables on the value of k_d for both processes (%)

Neural network	Parameters					
	$[H_2O_2]$	[Fe(II)]	[RB4]	$[(COOH)_2]$	pH	Temperature
Solar photo-Fenton	20.26	31.36	7.15	–	32.56	8.68
Solar photo-Fenton–ferrioxalate	5.10	31.51	–	27.94	28.14	7.31

Table 4
Reactions and constants for photo-Fenton degradation of RB4 (from ref. [8])

No.	Reaction	Rate constant (l mol s^{-1})
1	$Fe^{(II)} + H_2O_2 \rightarrow Fe^{(III)} + {}^{\bullet}OH + OH^-$	63
2	$Fe^{(II)} + {}^{\bullet}OH \rightarrow Fe^{(III)} + OH^-$	3×10^8
3	$H_2O_2 + {}^{\bullet}OH \rightarrow HO_2{}^{\bullet} + H_2O$	3.3×10^7
4	$Fe^{(II)} + HO_2{}^{\bullet} \rightarrow Fe^{(III)}(HO_2)^{+2}$	1.2×10^6
5	$HO_2{}^{\bullet} \rightarrow O_2{}^{-\bullet} + H^+$	1.58×10^5
6	$O_2{}^{-\bullet} + H^+ \rightarrow HO_2{}^{\bullet}$	1×10^{10}
7	$Fe^{(II)} + O_2{}^{-\bullet} + H^+ \rightarrow Fe^{(III)}(HO_2)^{+2}$	1×10^7
8	$Fe^{(III)} + H_2O \rightarrow Fe^{(III)}(HO_2)^{+2} + H^+$	2×10^{-3}
9	$Fe^{(III)}(HO_2)^{+2} + H^+ \rightarrow Fe^{(III)} + H_2O$	0.645
10	$Fe^{(III)}(HO_2)^{+2} \rightarrow Fe^{(III)} + HO_2{}^{\bullet}$	2.7×10^{-3}
11	$Fe^{(III)} + HO_2{}^{\bullet} \rightarrow Fe^{(II)} + O_2 + H^+$	2×10^3
12	$Fe^{(III)} + O_2{}^{-\bullet} \rightarrow Fe^{(II)} + O_2$	5×10^7
13	$HO_2{}^{\bullet} + HO_2{}^{\bullet} \rightarrow H_2O_2 + O_2$	8.3×10^5
14	$HO_2{}^{\bullet} + O_2{}^{-\bullet} + H^+ \rightarrow H_2O_2 + O_2$	9.7×10^7
15	${}^{\bullet}OH + HO_2{}^{\bullet} \rightarrow H_2O + O_2$	7.1×10^{-9}
16	${}^{\bullet}OH + O_2{}^{-\bullet} \rightarrow OH^- + O_2$	1×10^{10}
17	${}^{\bullet}OH + {}^{\bullet}OH \rightarrow H_2O_2$	5.2×10^9
18	$H_2O_2 + h\nu \rightarrow 2{}^{\bullet}OH$	–

completely disappeared. Thus, addition of H_2O_2 in different stages could help to reach a higher mineralization grade.

3.2. Solar photo-Fenton–ferrioxalate process

Ferrioxalate complexes absorb strongly at longer wavelength (250–450 nm) generating Fe(II) with a high quantum yield. Thus it is expected that degradation of RB4 could be improved by addition of oxalic acid to the system to form ferrioxalate. Previous works [8] confirm that Fe(II) is converted into Fe(III) in a few minutes in the presence of hydrogen peroxide. Accordingly, the destruction of RB4 is basically a process catalyzed by Fe(III)–H_2O_2. The addition of oxalic acid would then produce ferrioxalate in solution.

The complete experimental design and variables range for this process is shown in Table 1. The intervals of variables were reduced according to the best results obtained in the preceding study (solar photo-Fenton). Previous tests showed that concentrations above 60 ppm of oxalic acid produce precipitates in wastewater so the concentration of this reactive was upper limited. The concentration of RB4 was always kept in 20 ppm.

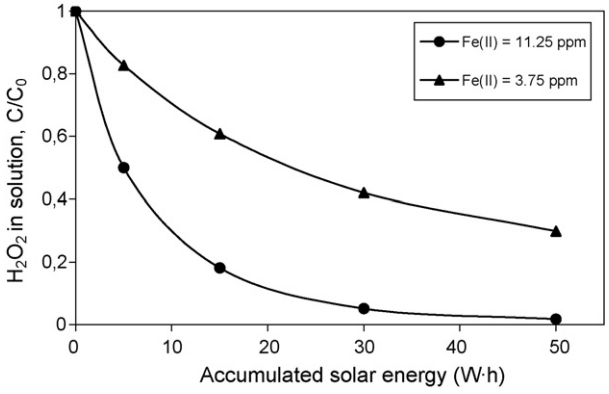

Fig. 4. Effect of initial Fe(II) concentration on hydrogen peroxide in solution for the solar photo-Fenton process (conditions: $[H_2O_2]$ = 150 ppm, [RB4] = 15 ppm, pH 4.5, T = 20 °C).

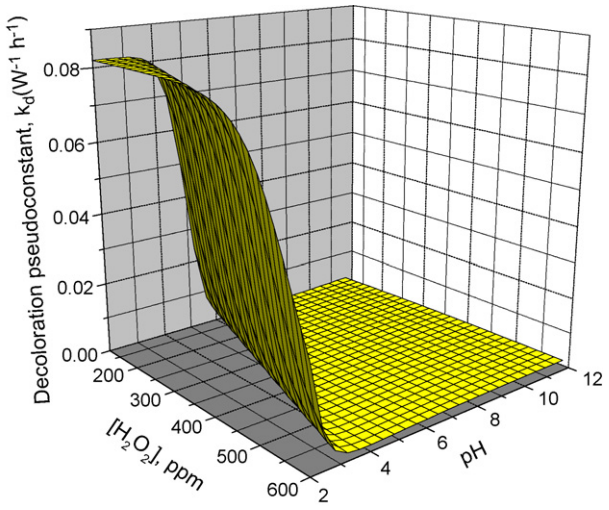

Fig. 5. NNs simulation of the effect of pH and $[H_2O_2]$ on the value of the decoloration rate pseudoconstant, k_d, for the solar photo-Fenton process (conditions: [Fe(II)] = 11.25 ppm, [RB4] = 20 ppm, T = 20 °C).

Experimental results and NNs fitting are shown in Fig. 2b and are in good agreement, with an average error lower than 14% for the decoloration rate pseudoconstant (k_d). The equation and parameters for the fitting using NNs are shown in Table 2.

The results of a saliency analysis on the input variables for each neural network (%) are shown in Table 3. In this case, pH, $[(COOH)_2]$ and [Fe(II)] are the most significant factors affecting the decoloration kinetics of the process, as will be explained below.

3.2.1. Effect of pH and H_2O_2 initial concentration

Fig. 7 simulates the effect of the initial concentration of hydrogen peroxide and pH on the kinetic decoloration rate pseudoconstant (initial conditions: T = 27 °C, [Fe(II)] = 7ppm, $[(COOH)_2]$ = 40). These results are in agreement with previous studies which have reported that when pH is lower than 3–4, the main Fe(III) species are $[Fe(C_2O_4)_2]^-$ and $[Fe(C_2O_4)_3]^{-3}$ which are highly photoactive [33,34]. However, when the pH value is increase to about 4–5, Fe(III)-oxalate species are mainly $Fe(C_2O_4)^+$ and $[\equiv Fe((C_2O_4)]^+$ which are low photoactive, resulting in a lower decoloration pseudoconstant.

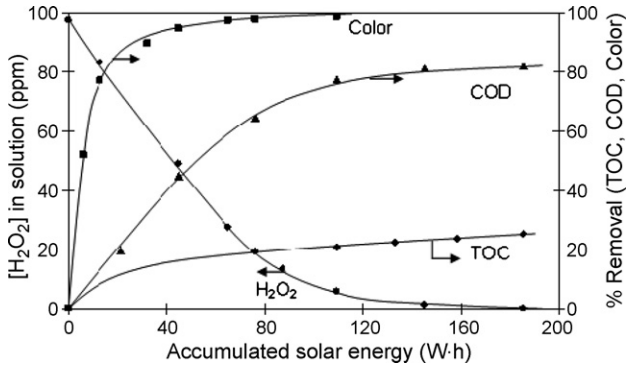

Fig. 6. Evolution of color, TOC, COD and H_2O_2 in solution under the optimum conditions for the solar photo-Fenton process (conditions: ($[H_2O_2]$ = 100 ppm, [Fe(II)] = 9 ppm, [RB4] = 25 ppm, pH 2).

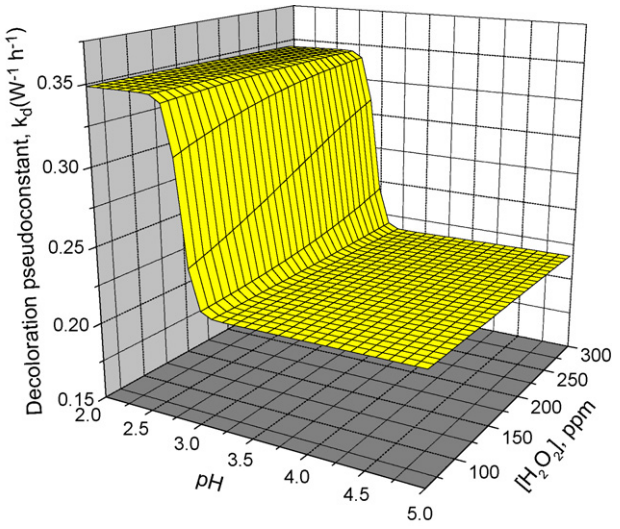

Fig. 7. NNs simulation of the effect of pH and initial concentration of hydrogen peroxide on the kinetic decoloration rate pseudoconstant for the solar photo-Fenton–ferrioxalate process (conditions: T = 27 °C, [Fe(II)] = 7 ppm, [$(COOH)_2$] = 40 ppm).

The initial concentration of H_2O_2 has a negligible effect into the experimental range as already reflected in Table 3 (5.1% in saliency analysis), since this specie is already formed during the photo-oxidation process in the presence of ferrioxalate, according to:

$$[Fe(C_2O_4)_3]^{3-} + h\nu \rightarrow Fe(II) + 2C_2O_4^{2-} + C_2O_4^{\bullet -} \quad (4)$$

$$C_2O_4^{\bullet -} + [Fe(C_2O_4)_3]^{3-} \rightarrow Fe(II) + 3C_2O_4^{2-} + 2CO_2 \quad (5)$$

$$C_2O_4^{\bullet -} + O_2 \rightarrow O_2^{\bullet -} + 2CO_2 \quad (6)$$

$$O_2^{\bullet -} + H^+ \rightarrow HO_2^{\bullet} \quad (7)$$

$$HO_2^{\bullet} + HO_2^{\bullet} \rightarrow H_2O_2 + O_2 \quad (8)$$

$$H_2O_2 + Fe^{(II)} \rightarrow Fe^{(III)} + {}^{\bullet}OH + OH^- \quad (9)$$

3.2.2. *Effect of $(COOH)_2$ and Fe(II) initial concentrations*

Fig. 8 shows (as an example) the effect of the initial concentration of oxalic acid and Fe(II) on the kinetic decoloration rate pseudoconstant at different temperatures into the experimental range as simulated by NNs (initial conditions: T = 27 or 35 °C, [H_2O_2] = 120 ppm, pH 2.5).

When the medium temperature of the test is 27 °C (Fig. 8a), the maximum degradation rate is reached at [$(COOH)_2$] $\geq$ 40 ppm and [Fe(II)] = 7 ppm, which corresponds with a mole ratio $(COOH)_2$:Fe close to 3, that is in agreement with Eq. (4).

However, when temperature reaches 35 °C (due to ambient conditions), results in Fig. 8b show that the RB4 degradation was increased with the increase of oxalic acid concentration, but it was inhibited with an excessive amount of acid. This behaviour was already found by other authors with different compounds [20,34]. There is an optimal initial concentration of oxalic acid and Fe(III) leading to the maximum constant. In this case, the maximum is found when [$(COOH)_2$] = 20 ppm and [Fe(II)] = 7 ppm (mole ratio $(COOH)_2$:Fe close to 2). It is possible that under these temperature conditions, more Fe(III) is converted into Fe(II), decreasing the former concentration and favoring the formation of $[Fe(C_2O_4)_2]^-$ which would be the main Fe(III)-oxalate specie present in solution.

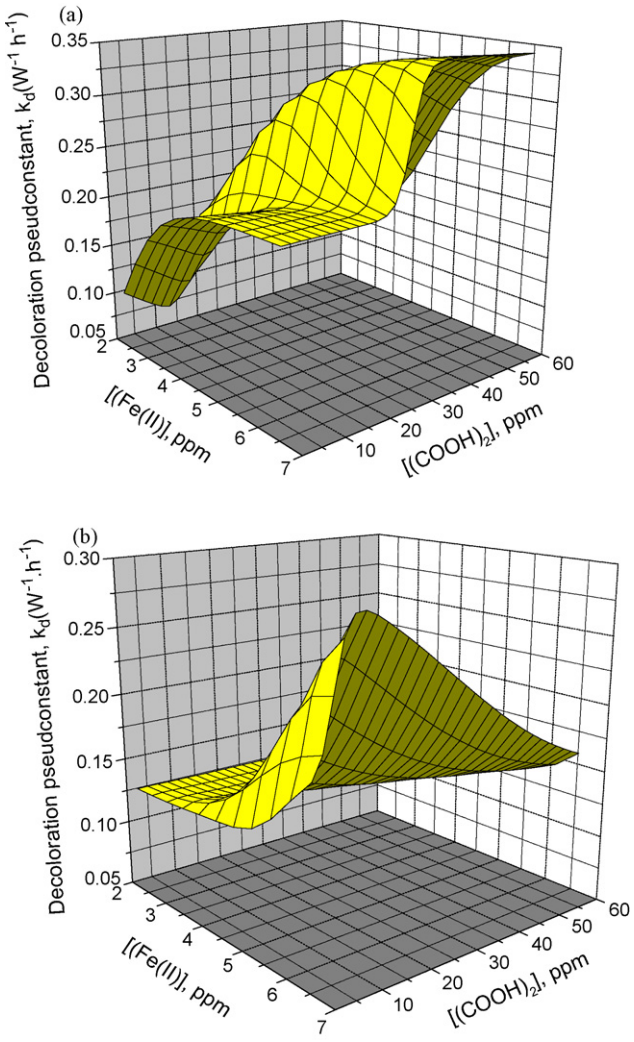

Fig. 8. NNs simulation of the effect of the initial concentration of oxalic acid and Fe(II) on the kinetic decoloration rate pseudoconstant for the solar photo-Fenton–ferrioxalate process. (a) Conditions: T = 27 °C, [H_2O_2] = 120 ppm, pH 2.5; (b) Conditions: T = 35 °C, [H_2O_2] = 120 ppm, pH 2.5.

On the other hand, in the Fe(III)-oxalate solutions, as the fraction of Fe(III) present as $[Fe(C_2O_4)_3]^{-3}$ decreases, a lower fraction of $C_2O_4^{\bullet -}/CO_2^{\bullet -}$ reacts with O_2 rather than with Fe(III) and consequently the formation rates and concentrations of the O_2-derived oxidants decrease [18], with the consequent decrease in the kinetic pseudoconstant, as observed in Fig. 8 (its maximum value decreases from 0.34 W^{-1} h^{-1} at 27 °C to 0.24 W^{-1} h^{-1} at 35 °C).

3.2.3. *Mineralization under the optimum conditions (solar-Fenton–ferrioxalate)*

A long experiment monitoring TOC, COD, color and H_2O_2 in solution was made under the optimum conditions selected from NNs ([H_2O_2] = 120 ppm, [Fe(II)] = 7 ppm, [$(COOH)_2$] = 10 ppm, pH 2.5). This test was made adding a new dose of

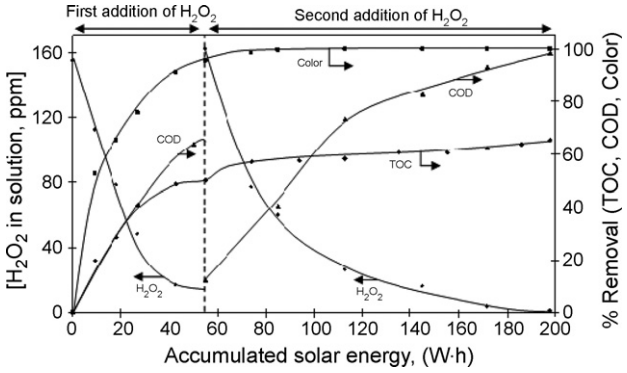

Fig. 9. Evolution of color, TOC, COD and H_2O_2 in solution under the optimum conditions for the solar photo-Fenton–ferrioxalate process (conditions: ($[H_2O_2]$ = 120 ppm,[Fe(II)] = 7 ppm, $[(COOH)_2]$ = 10 ppm, pH 2.5).

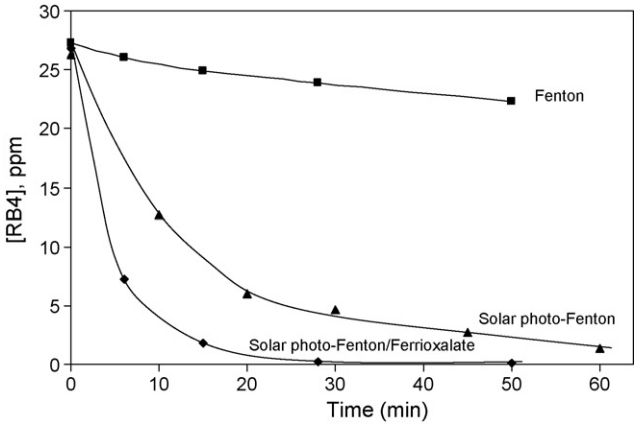

Fig. 10. Comparison of different processes (photochemical and not). Conditions: ($[H_2O_2]$ = 120 ppm, [Fe(II)] = 7 ppm, pH 2.5 and $[(COOH)_2]$ = 10 ppm (for solar photo-Fenton–ferrioxalate)).

hydrogen peroxide with the same concentration when the accumulated solar energy reached 55 W h. Results are shown in Fig. 9. Total decoloration and COD removal were obtained, whereas only 66% of TOC was removed. It is deduced that the second addition has a small effect on TOC reduction as previously commented.

3.3. Comparison of both processes

Finally, Fig. 10 summarizes a comparative study of both processes (together with the classic Fenton system) for the optimum conditions obtained under the best conditions in this research ($[H_2O_2]$ = 120 ppm, [Fe(II)] = 7 ppm, $[(COOH)_2]$ = 10 ppm, pH 2.5). It can be concluded that photochemical processes under a CPC solar reactor improves degradation and mineralization rates. The solar photo-Fenton–ferrioxalate process (with addition of oxalic acid) is a very favorable technique to degrade RB4 solutions.

4. Conclusions

- Results showed that acidic pHs (2–3) are more favorable for a faster decoloration process (higher decoloration kinetic rate pseudoconstant) for both processes: solar photo-Fenton and solar photo-Fenton–ferrioxalate.
- Solar photo-Fenton process: k_d increases with initial Fe(II) concentration until reaching a maximum value when a low concentration of H_2O_2 is used (<300 ppm). The amount of H_2O_2 remaining in solution is always very high when initial concentration of Fe(II) is low (3.25 ppm), showing that this reactive is in excess causing the known scavenger effect.
- Solar photo-Fenton process: under optimum conditions selected from NNs, 100% decoloration was obtained, but only 82% and 23% of COD and TOC removal respectively were reached. However, when the accumulated energy is 150 W h, hydrogen peroxide in solution has disappeared completely.
- The solar photo-Fenton–ferrioxalate process increases degradation rate of RB4 since ferrioxalates absorbs strongly and a higher portion of the solar spectrum can be used. The addition of oxalic acid increases overall operating costs, but it also helps to reduce pHs in solution. Under the optimum conditions, ($[H_2O_2]$ = 120 ppm in two additions, [Fe(II)] = 7 ppm, $[(COOH)_2]$ = 10 ppm, pH 2.5), total decoloration and COD removal were achieved whereas 66% of TOC was eliminated.

Acknowledgements

Financial support from the Consejería de Educación y Ciencia of the Junta de Comunidades de Castilla-La Mancha (PAI06-0050-2582) and the University of Castilla-La Mancha (Emergent Groups Program) is gratefully acknowledged.

References

[1] H. Park, W. Choi, J. Photochem. Photobiol. A159 (2003) 241–247.
[2] P.A. Carneiro, R.F. Pupo Nogueira, M.V.B. Zanoni, Dyes Pigments 74 (2007) 127–132.
[3] N. Deng, F. Luo, F. Wu, M. Xiao, X. Wu, Water Res. 34 (2000) 2408–2411.
[4] B. Neppolian, H.C. Choi, S. Sakthivel, B. Arabindoo, V. Murugesan, J. Hazard. Mater. 89 (2002) 303–317.
[5] B. Neppolian, H.C. Choi, S. Sakthivel, B. Arabindoo, V. Murugesan, Chemosphere 46 (2002) 1173–1181.
[6] P.A. Carneiro, N. Boralle, N.R. Stradioto, M. Furlan, M.V.B. Zanoni, J. Braz. Chem. Soc. 15 (2004) 587–594.
[7] P.A. Carneiro, M.E. Osugi, C.S. Fugivara, N. Boralle, M. Furlan, M.V.B. Zanoni, Chemosphere 59 (2005) 431–439.
[8] A. Durán, J.M. Monteagudo, M. Mohedano, Appl. Catal. B: Environ. 65 (2006) 127–134.
[9] M. Neamtu, A. Yediler, I. Siminiceanu, A. Kettrup, J. Photochem. Photobiol. A 161 (2003) 87–93.
[10] S. Malato, J. Blanco, J. Cáceres, A.R. Fernández-Alba, A. Agüera, A. Rodríguez, Catal. Today 76 (2002) 209–220.
[11] S. Malato, J. Blanco, M.I. Maldonado, P. Fernández, D. Alarcón, M. Collares, J. Farinha, J. Correia de Oliveira, Solar Energy 77 (2004) 513–524.
[12] J. Blanco, S. Malato, B. Millow, M.I. Maldonado, H. Fallmann, T. Krutzles, R. Bauer, J. Phys. IV 9 (1999) 259–264.
[13] R.F.P. Nogueira, A.G. Trovó, D.F. Mode, Chemospere 48 (2002) 385–391.
[14] R. Bauer, G. Waldner, H. Fallmann, S. Hager, H. Karé, T. Krutzler, S. Malato, P. Maletzky, Catal. Today 53 (1999) 131–144.
[15] M.S. Lucas, J.A. Peres, Dyes Pigments 74 (2007) 622–629.

[16] A. Safarzadeh-Amiri, J.R. Bolton, S.R. Cater, Water Res. 31 (1997) 787–798.
[17] K. Selvam, M. Muruganandham, M. Swaminathan, Solar Energ. Mat. Sol. C 89 (2005) 61–74.
[18] B.C. Faust, R.G. Zepp, Environ. Sci. Technol. 27 (1993) 2517–2522.
[19] Y.H. Huang, S.T. Tsai, Y.F. Huang, C.Y. Chen, J. Hazard. Mater. 140 (2007) 382–388.
[20] F.B. Li, X.Z. Li, C.S. Liu, X.M. Li, T.X. Liu, Ind. Eng. Chem. Res. 46 (2007) 781–787.
[21] G.E.P. Box, W.G. Hunter, J.S. Hunter, Statistics for Experimenters: An Introduction to Design, Data Analysis and Model Building, Wiley, New York, 1978.
[22] D.P. Morgan, C.L. Scofield, Neural Networks and Speech Processing, Kluwver Academic Publishers, London, 1991.
[23] D.W. Marquardt, J. Soc. Ind. Appl. Math. 11 (1963) 431–441.
[24] B. Nath, R. Rajagopalan, R. Ryker, Comput. Oper. Res. 24 (1997) 767–773.
[25] F.J. Beltrán, M. González, F.J. Rivas, P. Alvarez, Water Air Soil Pollut. 105 (1998) 685–700.
[26] J. Jeong, J. Yoon, Water Res. 39 (2005) 2893–2900.
[27] D.L. Sedlak, A.W. Andren, Environ. Sci. Technol. 25 (1991) 777–782.
[28] E. Lipczynska-Kochany, Proceedings of the Third International Symposium Chemical Oxidation. Technology of the Nineties Vol. 3, Technomic Publishing Co., Lancaster, Pensylvania (1993), pp. 12-27.
[29] J.W. Moffett, R.G. Zika, Environ. Sci. Technol. 21 (1987) 804–810.
[30] S.H. Bossmann, E. Oliveros, S. Göb, M. Kantor, A. Göppert, L. Lei, P.L. Yue, A.M. Braun, Water Sci. Technol. 44 (2001) 257–262.
[31] W.J. Epolito, Y.H. Lee, L.A. Bottomley, Dyes Pigments 67 (2005) 35–46.
[32] G. Sagawe, A. Lehnard, M. Lübber, D. Bahnemann, Helv. Chim. Acta 84 (2001) 3742–3759.
[33] M.E. Balmer, B. Sulzberger, Environ. Sci. Technol. 30 (1999) 2418–2424.
[34] F.B. Li, X.Z. Li, X.M. Li, T.X. Liu, J. Dong, J. Colloid Interface Sci. 311 (2007) 481–490.